Unintended consequences of climate change mitigation for African river basins

Matteo Giuliani[1], Jonathan R. Lamontagne[2], Mohamad I. Hejazi[3,4], Patrick M. Reed[5], Andrea Castelletti[1]

(1) Department of Electronics, Information, and Bioengineering Politecnico di Milano, Milano, Italy.

(2) Department of Civil and Environmental Engineering, Tufts University, Medford, MA.

(3) Joint Global Change Research Institute, Pacific Northwest National Laboratory, College Park, MD.

(4) King Abdullah Petroleum Studies and Research Center (KAPSARC), Riyadh, Saudi Arabia.

(5) School of Civil and Environmental Engineering, Cornell University, Ithaca, NY.

Emerging climate change mitigation policies focus on the implementation of global measures relying on carbon prices to attain rapid emissions reductions, with limited consideration for the impacts of global policies at local scales. Here, we use the Zambezi Watercourse in Southern Africa to demonstrate how local dynamics across interconnected Water-Energy-Food (WEF) systems are impacted by mitigation policies. Our results indicate that climate change mitigation policies related to land-use change emissions can have negative side effects on local water demands, generating increased risks for failures across all the components of the WEF systems in the Zambezi Watercourse. Analogous vulnerabilities could impact many river basins in Southern and Western Africa. It is critical to connect global climate change mitigation policies to local dynamics for a better exploration of the full range of possible future scenarios while supporting policy makers in prioritizing sustainable mitigation and adaptation solutions.

The 2015 Paris Agreement on Climate Change introduced ambitious global commitments to mitigate climate change and limit the global temperature increase to 1.5-2°C above pre-industrial levels. The recent scientific literature suggests that achieving these targets will require immediate and rapid emissions reductions [1], with promising emerging pathways that combine high carbon prices in the near term [2] with the deployment of net negative emission technologies in the second half of the century [3]. Integrated Assessment Models (IAMs) are widely used to evaluate the efficacy and impact of these measures across a range of possible future scenarios [4, 5, 6] that attempt to capture the complex interactions of energy, land-use, economic, water, and climate systems. These studies generally develop global [6] or regional analyses [7] relying on economic abstractions of global welfare preferences, with less attention paid to the quantification of local-scale impacts of abatement options for diverse groups of stakeholders with potentially conflicting needs or preferences [8].

This paper addresses this gap by investigating how multisector dynamics across interconnected Water-Energy-Food (WEF) systems at the local scale are impacted by global climate change mitigation policies. Our analysis uses a river basin-scale model of the Zambezi Watercourse (ZW) in Southern Africa that enables exploration of synergies, tradeoffs, and vulnerabilities for the WEF systems including hydropower production, irrigation supply, and ecosystem services in one of the largest transboundary river basins in Africa as well as in the world. The rapid economic development of the region is increasing both energy and water demands, triggering major investments in hydropower development and the expansion of irrigated agriculture. These trends make the ZW an emblematic example of most river basins in developing countries that now must find a balance between social, economic, and environmental interests to promote development pathways that are inclusive as well as environmentally and economically sustainable [9].

While previous studies [10, 11, 12, 13] have primarily investigated the local impacts of climate change and regional development plans, here we expand the scope of the analysis to explore the interactions of climate change with global socio-economic teleconnections by considering a large ensemble of global scenarios simulated by the Global Change Analysis Model (GCAM [14]), a model widely used in major integrated climate-energy-economic assessments [15, 16, 17]. To explore the uncertainty space, we adopt an exploratory modeling approach to systematically sample the Shared

Socioeconomic Pathways (SSPs [18]) components along with multiple Shared Policy Assumptions (SPAs [19]) that set a mitigation policy context, including regional participation in mitigation efforts and the pricing of carbon emissions [20], resulting in 33,750 scenarios [21] (see Methods). Specifically, those scenarios include detailed, regionally specific and globally contextualized descriptions of population and economic growth, technological change, and climate change mitigation policy fragmentation drawn from the SSP/SPA implementation in GCAM [17]. The resulting scenario database contains tens of thousands of self-consistent, multi-sector, multi-scale, time-evolving scenarios of hundreds of climate, economic, demographic, and land-use variables. We spatially and temporally downscale the GCAM outputs [22] to generate projections of local irrigation demands at the basin scale [23]. We also bias-adjust climate projections from different combinations of global and regional climate models for different Representative Concentration Pathways (RCPs, [24]) to force local hydrological models and produce projections of water availability. To ensure the consistency of the projected scenarios, we focus our analysis on an ensemble of scenarios that couple a projection of water availability driven by one RCP with a sub-set of projected irrigation demands based on the end-of-century radiative forcing as simulated by GCAM (see Methods). We first explore the synergies and trade-offs across the WEF systems by analyzing a set of alternative adaptive operating policies for managing major reservoirs and irrigation diversions in the basin under observed climate and irrigation demands, showing that hydropower generation and irrigation supply are not strongly in conflict today. However, our projections suggest the ZW will be exposed to severe risks of performance degradation across all the components of the WEF systems. Our results demonstrate these future vulnerabilities are mostly generated by global socio-economic drivers, namely the alternative land-use change policies, rather than predicted changes in water availability due to climate change. Analogous vulnerabilities are found across most basins in Southern and Western Africa, raising concerns about the equity of these global climate change mitigation policies for African countries.

The WEF Nexus in river basins under development

Africa has more than 60 international river basins that are a primary factor in the location and production patterns of human settlements as well as in the structure and productivity of African economies [25]. At the same time, African rivers, lakes, and wetlands are a major biodiversity reserve providing a large variety of ecosystem services, ranging from fishing and flood-recession agriculture to habitats for wildlife, migratory birds, and endemic species of global conservation concern [26]. In many countries, however, the accelerated population growth and the fast-economic development are motivating large-scale infrastructure investments to meet increasing water, energy, and food demands [27, 28, 29]. These projects may constitute a major threat to natural ecosystems and local subsistence needs [30]. In these evolving contexts, a major challenge to policy makers is navigating the tradeoffs of alternative development pathways between competing multisector dynamics, across different spatial scales, and over different time horizons including a broad array of potential climate, socio-techno-economic, and policy futures [31].

The ZW is a typical example of river basins under development. From the headwaters in northwest Zambia, the river flows eastward for 2,750 km, also receiving water from the Kafue, Luangwa, and Shire rivers, draining a catchment area of 1.39 million km^2 shared by eight countries, namely Angola, Botswana, Malawi, Mozambique, Namibia, Tanzania, Zambia, and Zimbabwe (Figure 1). The basin provides services to a population of 40 million people, which is expected to grow rapidly up to 70 million by 2050 [32]. The high runoff in the upper part of the basin combined with a change in elevation of more than 1000 m along the river's course to the ocean provides significant potential for hydropower energy production. The current installed capacity is about 5.5 GW, with an additional 8.4 GW planned by the end of 2023 [33]. Around 70% of this installed capacity is concentrated in two mega-dams, namely Kariba (1,830 MW) and Cahora Bassa (2,075 MW). Existing irrigated areas cover about 182,000 ha with an annual water demand exceeding 6,300 Mm^3/y (the average monthly demand is 525.6 Mm^3/month, with a peak close to 1051 Mm^3/month), and the planned expansion will add other 336,000 ha [27]. Major cultivated crops are sugar cane (23%), rice (17%), wheat (15%), and maize (14%) [11]. The ZW also provides numerous ecosystem services, which are being endangered by the development of hydropower and irrigated agriculture. These services include 82

key biodiversity areas [34], numerous fisheries that represent the main source of proteins for the local rural communities, and tourism primarily to Victoria Falls and other national parks that generate around 10 million US$/year [27]. Moreover, the basin comprises several wetlands of international importance, including an extensive alluvial plain in the Zambezi Delta covering approximately 1.2 million ha [26], where observed flows during the flooding season have been strongly reduced after the completion of Cahora Bassa with respect to the pre-dam conditions [35]. This trend is expected to further worsen because of the planned dam construction and irrigated agriculture expansions.

Future vulnerabilities across the WEF systems

Given the ZW model and the local objectives for the WEF systems defined in collaboration with local stakeholders (see Methods and Supplementary Sections S1 and S2), we first perform a multisectoral analysis on a set of 121 alternative operating policies for managing existing reservoirs and irrigation diversions that capture the optimal tradeoffs (i.e., Pareto efficient [36]) across their competing multi-sectoral demands over historically observed conditions. Each Pareto-optimal control solution represents a different balance of compromises across the WEF objectives (Supplementary Figure S1). The maximization of hydropower production negatively impacts environmental conditions in the Delta (Supplementary Figure S2). The tradeoff between energy and irrigation supply is in turn weak and allows moving from a maximum deficit equal to 88.5 m^3/s to 21.7 m^3/s by accepting a 0.80 TWh/y reduction in hydropower production, which means a 75% improvement at the cost of a 3% reduction in hydropower. Similar to previous results [37], our analysis suggests that the system's historical operations emphasize the maximization of hydropower production, under which existing irrigation demands are mostly satisfied. Yet, a key question is whether multi-sector resource conflicts may become more severe in future scenarios that have either climate-induced decreases in water availability, population-driven increases in irrigation demand, an intensification of agricultural activities in the region, or a combination of the three.

To investigate the future vulnerabilities of the modeled historical operations of the ZW system (see Supplementary Figure S1) to these potential conflicts, we sample six socio-economic uncertainties as represented in the SSPs and simulated using GCAM (see Methods). Those socio-economic scenarios were paired with three climate projections corresponding to downscaled and bias-adjusted RCP2.6, RCP4.5, and RCP8.5 scenarios. To ensure consistency between the socio-economic and climate scenarios, the coupling was performed based on the 2100 radiative forcing projected within GCAM (see Supplementary Figure S3). This coupling resulted in an ensemble of 7,317 interdependent scenarios (see Methods for details). For each RCP, the differences in the underlying irrigation demands introduce large variability in system performance. Reduction in hydropower production (Figure 2a) appears mostly driven by the projected decreases in water availability. Similar to previous research [13, 11], the median estimated production under RCP2.6 and RCP4.5 lie in the range of 15% to 25% decrease relative to the historical production (i.e., 20.16 TWh/y), while registering a 40% decrease under RCP8.5. Similar patterns emerge with respect to the different climate models' chains: the highest levels of hydropower production attained in each RCP are obtained using the projections characterized by the highest precipitation (Supplementary Figure S5) that produce the highest streamflows (Supplementary Figure S6). The temperature projections are instead consistent across the climate model chains (Supplementary Figure S4). The median simulated value of irrigation deficit (Figure 2b) is also largely dependent on the climate scenarios, with significantly higher deficits under RCP8.5 (i.e., more than 7 times higher than the historical value) than under the other two climate scenarios. However, both the worst first percentile of hydropower production and the worst tenth percentile of irrigation deficit are registered under RCP4.5. Lastly, the projected performance in terms of environmental deficit (Figure 2c) shows an overall worsening of about 22% with respect to the performance under historical conditions across all scenarios, with the simulated values of flow deficits that correspond to about one third of the flow target in the Zambezi Delta. Interestingly, the median values of environmental deficit for the different RCPs are not ordered according to the predicted annual flow entering the river basin. The best performance is indeed obtained under RCP2.6, but the worst performance is obtained under RCP4.5 rather than under RCP8.5, which is the climate scenario with the lowest projected natural water availability.

Discovering the global drivers of local vulnerabilities

The unexpected vulnerabilities under RCP4.5 (Figure 2) suggest that the socio-economic scenarios and mitigation regimes associated with this climate projection play a major role in determining the future system dynamics. To infer the key controls of such dynamics, the scatterplot in Figure 3a explores the growth of crop water consumption in Southern Africa simulated by GCAM across a wide ensemble of socio-economic scenarios, with colors distinguishing alternative policies of Land Use Change (LUC) emissions prices (see Supplementary Figure S7 for disaggregated irrigation water growth). As implemented by [21, 17], the LUC emissions price is represented as a fraction of the underlying carbon price. We tested two LUC price regimes: a regionally differentiated and a globally uniform LUC price (roughly consistent with SPAs 4 and 2, respectively). In the regionally differentiated case, wealthy countries make strong attempts to curb LUC emissions, as represented by a high LUC emissions price, while developing countries have limited LUC policies represented by a lower LUC emissions price (see Supplementary Figure S13). As a baseline, we also consider a case with no emissions price of any kind implemented.

Our results show that emissions prices are effective at impacting the level of GHG emissions and the resulting end of century radiative forcing, but also that the nature of the LUC prices produce three clusters of regional crop water consumptions. Scenarios with no emissions price of any kind result in values of radiative forcing in the range 6-10 W/m^2 that are associated with the RCP8.5 scenario (red distributions in Figure 2), with an average projected crop water consumption increase of about 300%. The application of a price on emissions successfully contains the radiative forcing below 7 W/m^2, with many of these scenarios that are hence compatible with the RCP4.5 climate projections (green distributions in Figure 2). The scenarios with the lowest 2100 forcing are instead associated with the RCP2.6 scenario (blue distributions in Figure 2). While the scenarios emissions prices successfully limit the overall end-of-century radiative forcing, we found the nature of the LUC price regime can have a significant impact on regional land-use changes.

In GCAM, land use and cropping decisions are made on an economic basis (see Supplementary Section S3). Regions that have some advantage for a particular use (due to climate, technology, etc.) will attract more of that use. When a LUC emissions price is in place, the carbon intensity of any land use change factors into the economic decision of where different crops are grown. A fragmented LUC emissions price makes non-participating regions, like Southern Africa in our study, more favorable to agricultural expansion, and this dynamic explains the significant influence the type of LUC emissions price has on Southern African agricultural water use. As described in Supplementary Section S3, the exact magnitude of this effect depends on dozens of other factors, but it is a robust phenomenon observed across the ensemble. All else held equal, fragmented LUC policies tend to concentrate new development where land use change is not priced as high, and this effect leads to between 50 and 300 Mt of additional crop production in Southern Africa (Supplementary Figure S20). The exact composition of this additional production depends heavily on scenario factors and varies widely across the ensemble, but in general the large increases occur in corn, root tuber, sugar crop (for food), and miscellaneous crops (nuts and fruits).

One interpretation is that the LUC price fragmentation produces favorable conditions for land grabbing practices [38], with wealthy countries investing in the realization of extensive agricultural projects (e.g., large scale, intensive irrigation projects similar to the existing Mazabuka district). Under this fragmented scenario, crop water consumption in Southern Africa (where the LUC emissions price is low) increases up to 700% due to extensive agricultural LUC, from the conversion of grass and shrublands, pasture, and other arable lands to new crop production. Conversely, the same scenarios under the globally uniform LUC price, representing a unified approach to LUC pricing, experience increases that do not exceed 300%, with virtually the same radiative forcing.

The scatterplot in Figure 3b confirms the key role of LUC emission policies by showing that the globally uniform LUC price produces a similar increase in crop water consumption between the Southern Africa region and the rest of the world. The regionally differentiated LUC price, instead,

introduces diverse responses with an increase in the Southern Africa region that is much larger than the global one. These scenarios explain the divergent distributions of the irrigation deficit under RCP2.6 and RCP4.5 (Figure 2b) which have similar conditions in terms of projected natural water availability. Moreover, high demands imply large water abstractions to serve the irrigation districts along the Zambezi River that reduce the water flowing into the Delta. This practice negatively impacts the ecosystem services provided by the Zambezi River Delta (Figure 2c), showing how the impact of future socio-economic conditions may offset the one of the projected climate conditions.

Discussion and Conclusions

Our study indicates that global climate change mitigation policies can have side effects on local water demands. Containing GHG emissions and the resulting end-of-century radiative forcing may prevent substantial reduction of water availability in a river basin but does not necessarily result in better system performance. We find that the Water-Energy-Food systems in the ZW are exposed to severe risks of performance degradation that are mostly generated by global socio-economic drivers, notably the alternative policies of land-use change prices. Since the ZW is representative of many river basins where large dams are planned to support growing economies, we expect our findings to be generalizable to several other African regions.

In our scenarios, the average continental increase of end of century crop water consumption relative to 2005 is equal to 140%, with diverse trends across the five African regions ranging from 395% and 152% increases in Southern and Northern Africa, respectively, to a 30% decrease in Eastern Africa (see Supplementary Figure S8). Notably, the consumption increase under regionally differentiated LUC emission price is about two times larger than under globally uniform LUC price for both the Southern and Western Africa regions (Figure 4). These two regions also include about 60% of all African dams currently planned or under construction [39]. These features suggest that both regions are expected to be exposed to increasing local demands and vulnerabilities comparable to the ones illustrated for the ZW case, which might be unintentionally underestimated by ignoring large-scale socio-economic dynamics in the attempt of enhancing the accuracy of local scale models [40]. At the same time, decoupling water demands from the analysis of global climate policies could misrepresent local multisector dynamics, not only in terms of projected water demands but also for electricity capacity expansion [41].

We should therefore better understand the tradeoff between targeting realism at the local scale and representing global socio-economic teleconnections to be able to explore the full range of possible future scenarios [42] when supporting policy makers in prioritizing mitigation and adaptation strategies across different spatial scales. Our finding highlights how well-intentioned climate change mitigation policies introduced in wealthier countries could have the unintended consequence of increasing vulnerabilities in river basins throughout the developing world. To avert these negative effects, policy makers may have to look beyond their borders to avoid water-use outsourcing and to ensure environmental and climate justice for all [43, 44].

Acknowledgements

The authors would like to thank Alessandro Amaranto, Barbara Benigni, Federica Bertoni, Abigail Birnbaum, Flannery Dolan, and Sebastian Raimondo for their contribution in developing initial numerical experiments. The authors would like to also thank Mr. Mutale (Executive Secretary of the Zambezi Watercourse Commission) for the feedbacks provided during the DAFNE project. Co-authors MG and AC have been partially supported by DAFNE under H2020 framework programme of the European Union, grant number 690268.

Author contributions

MG, JL, AC designed the research and writing of the paper. MG and JL conducted the numerical experiments and lead the data analysis. MH and PR contributed in analysis of results and writing of the paper.

Competing Interests.
The authors declare that they have no competing financial interests.

Correspondence
Correspondence and requests for materials should be addressed to Andrea Castelletti (email: andrea.castelletti@polimi.it).

Figure Captions

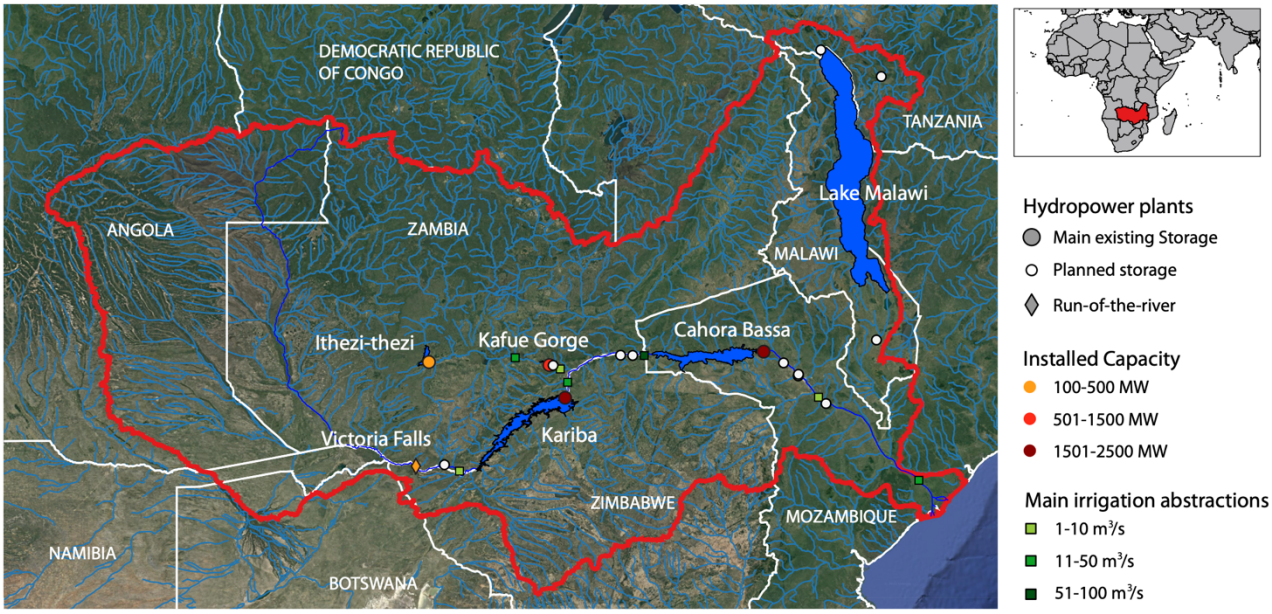


Figure 1: Locations of dams and irrigation districts in the Zambezi Watercourse. Four dams and six power plants are currently in operations for a total installed capacity of 5,500 MW, while existing irrigated areas cover about 182,000 ha.

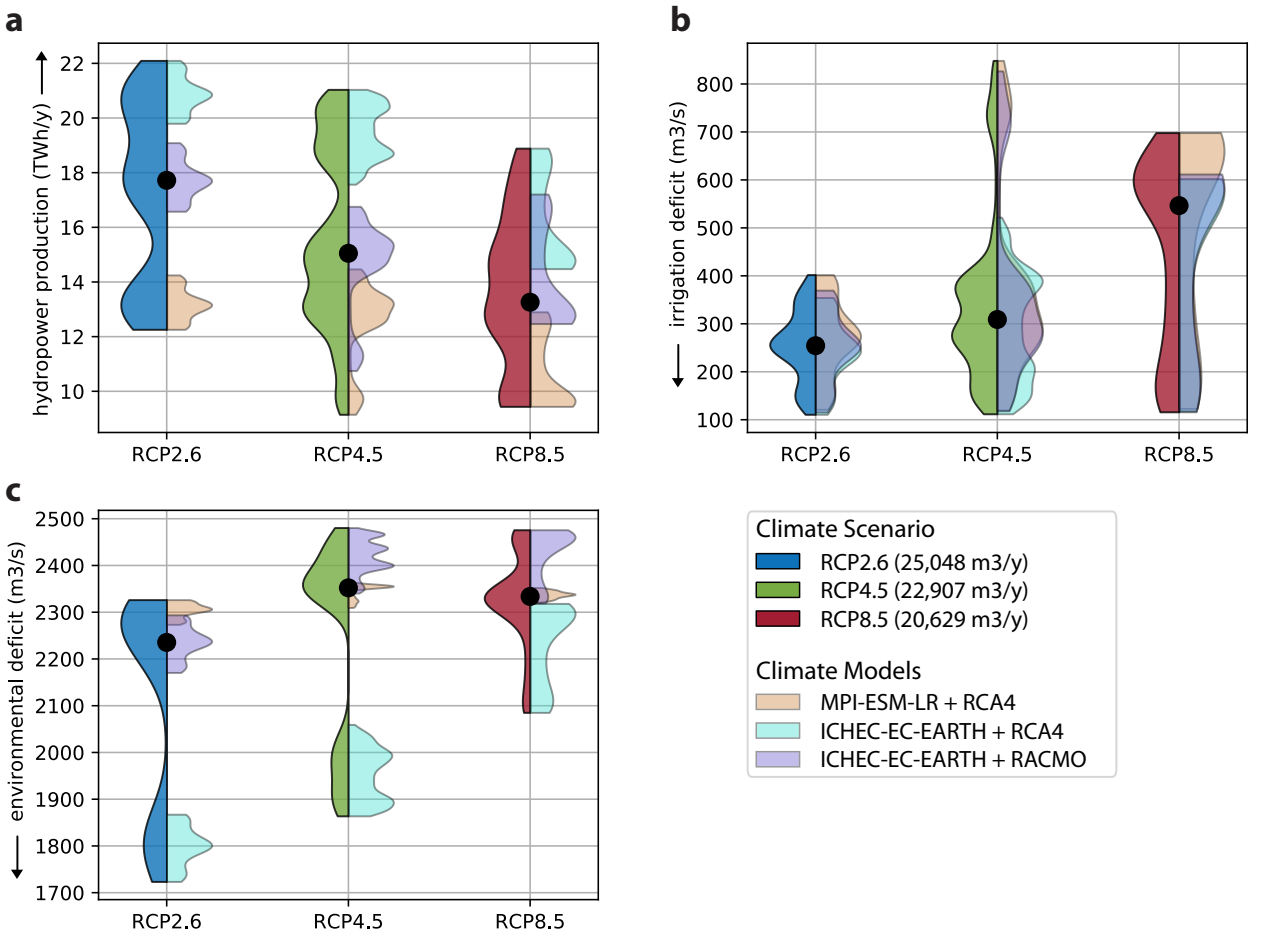


Figure 2: Future system vulnerabilities. Uncertain attainment of the local ZW objectives estimated via simulation of the modeled historical operations over the ensemble of interdependent climate and socio-economic scenarios. Violin plots show the statistical distribution of results for hydropower production (a), irrigation deficit (b), and environmental deficit (c), while the variance objective is not shown due to its limited sensitivity to the considered scenarios. Black arrows indicate the direction of increasing preference for each objective. Black circles indicate the median value for a specific RCP scenario across different irrigation demand scenarios. The left distributions show the multi-model results, which are disaggregated by climate models in the right distributions.

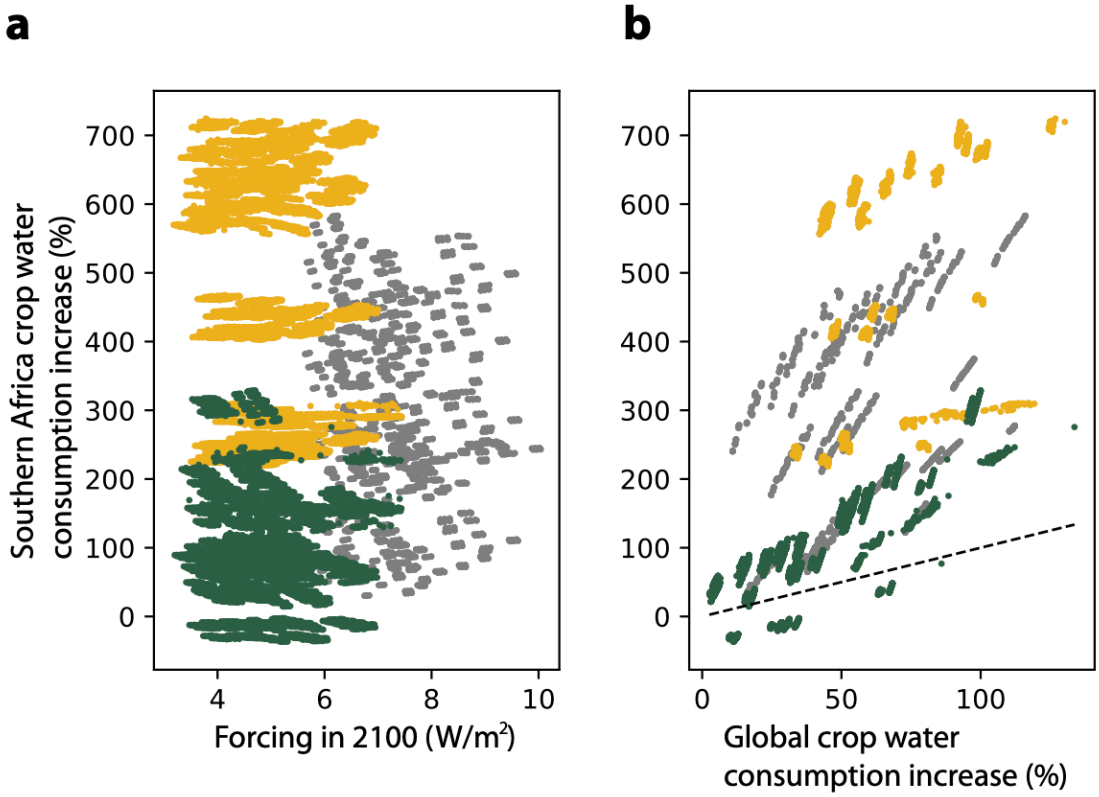


Figure 3: Analysis of socio-economic scenarios generated by GCAM. a, Scatterplot between end of century radiative forcing and crop water consumption growth relative to 2005 for the Southern Africa region. **b,** Scatterplot between global and Southern Africa crop water consumption growth relative to 2005 (the black dashed line is the 1:1 reference). Colors represent alternative policies of Land Use Change (LUC) emission price: gray points are scenarios with no emission price, green with globally uniform LUC price, and yellow with regionally differentiated LUC price (i.e., wealthy countries pay a higher LUC emission price than developing ones due to their strong attempts to curb LUC emission).

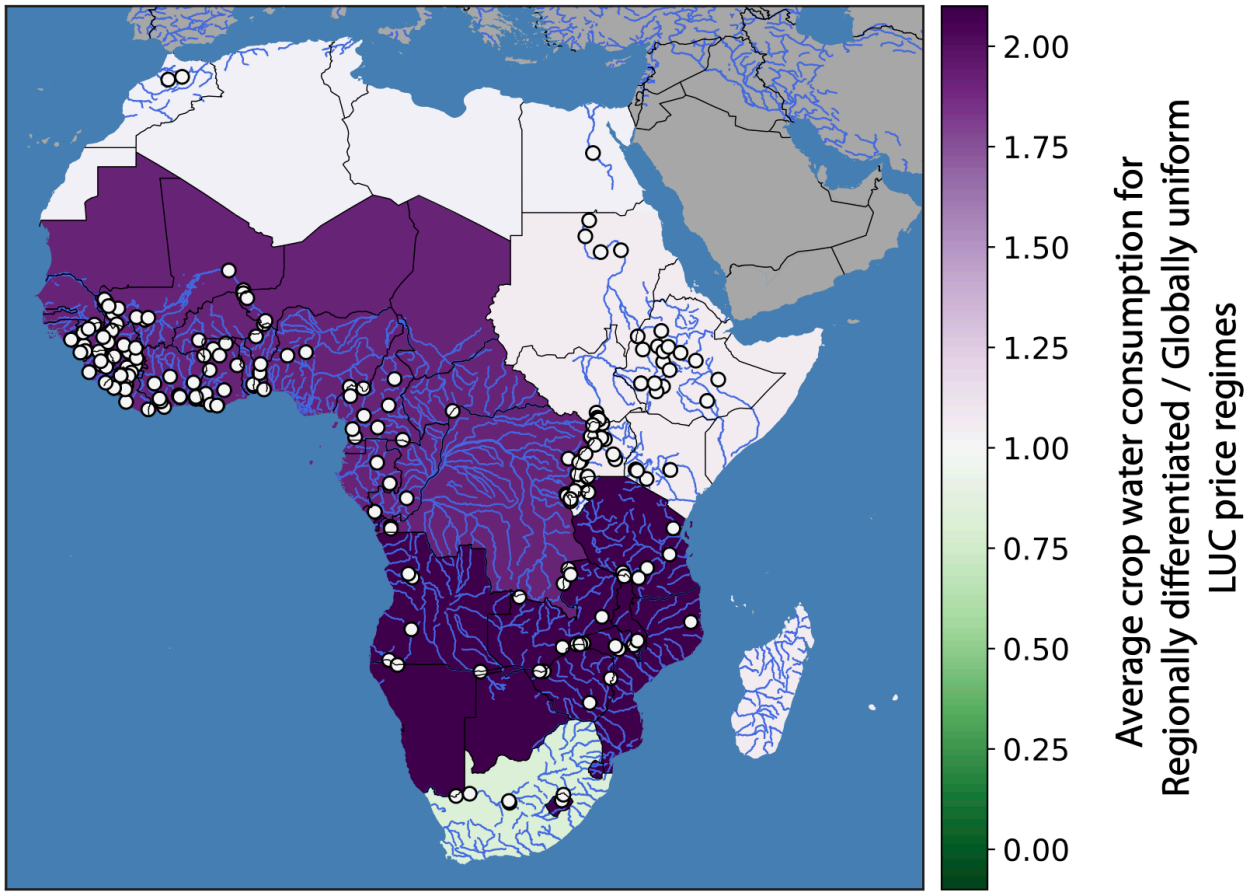


Figure 4: Projected vulnerabilities of African regions. The map shows African countries colored according to the ratio of average 2005-2100 crop water consumption projected by GCAM for scenarios with regionally differentiated LUC price over the one of scenarios with globally uniform LUC price. The white circles indicate the locations of future hydropower reservoirs and dams extracted from [39].

References

[1] J. Lamontagne, P. Reed, G. Marangoni, K. Keller and G. Garner, "Robust abatement pathways to tolerable climate futures require immediate global action," *Nature Climate Change,* vol. 9, no. 4, pp. 290-294, 2019.

[2] G. Luderer, Z. Vrontisi, C. Bertram, O. Y. Edelenbosch, R. C. Pietzcker, J. Rogelj, H. S. D. Boer, L. Drouet, J. Emmerling, O. Fricko, S. Fujimori, P. Havlík, G. Iyer, K. Keramidas and A. Kitous, "Residual fossil CO2 emissions in 1.5–2 C pathways," *Nature Climate Change,* vol. 8, no. 7, pp. 626-633, 2018.

[3] D. van Vuuren, A. Hof, M. van Sluisveld and K. Riahi, "Open discussion of negative emissions is urgently needed," *Nature Energy,* vol. 2, pp. 902-904, 2017.

[4] S. Santos Da Silva, F. Miralles-Wilhelm, R. Muñoz-Castillo, L. E. Clarke, C. J. Braun, A. Delgado, J. A. Edmonds, M. Hejazi, J. Horing, R. Horowitz, P. Kyle, R. Link, P. Patel, S. Turner and McJeon, "The Paris pledges and the energy-water-land nexus in Latin America: Exploring implications of greenhouse gas emission reductions," *PLoS One,* vol. 14, no. 4, 2019.

[5] S. Fujimori, T. Hasegawa, V. Krey, K. Riahi, C. Bertram, B. Leon Bodirsky, V. Bosetti, J. Callen, J. Després, J. Doelman, L. Drouet, J. Emmerling, S. Frank and Fricko, "A multi-model assessment of food security implications of climate change mitigation," *Nature Sustainability,* vol. 2, pp. 386-396, 2019.

[6] J. Rogelj, D. McCollum, B. O'Neill and K. Riahi, "2020 emissions levels required to limit warming to below 2° C," *Nature Climate Change,* vol. 3, no. 4, pp. 405-412, 2013.

[7] M. Tavoni, E. Kriegler, K. Riahi, D. Van Vuuren, T. Aboumahboub, A. Bowen, K. Calvin, E. Campiglio, T. Kober, J. Jewell, G. Luderer, G. Marangoni, D. McCollum, M. van Sluisveld and A. Zimmer, "Post-2020 climate agreements in the major economies assessed in the light of global models," *Nature Climate Change,* vol. 5, no. 2, pp. 119-126, 2015.

[8] G. Garner, P. Reed and K. Keller, "Climate risk management requires explicit representation of societal trade-offs," *Climatic Change,* vol. 134, pp. 713-723, 2016.

[9] J. Dearing, R. Wang, K. Zhang, J. Dyke, H. Haberl, M. Hossain, P. Langdon, T. Lenton, K. Raworth, S. Brown, J. Carstensen, M. Cole, S. E. Cornell, T. Dawson, C. Doncaster, F. Eigenbrod, M. Flörke, E. Jeffers and A. Mackay, "Safe and just operating spaces for regional social-ecological systems," *Global Environmental Change,* vol. 28, pp. 227-238, 2014.

[10] H. Kling, P. Stanzel and M. Preishuber, "Impact modelling of water resources development and climate scenarios on Zambezi River discharge," *Journal of Hydrology: Regional Studies,* vol. 1, pp. 17-43, 2014.

[11] R. Payet-Burin, M. Kromann, S. Pereira-Cardenal, K. Strzepek and P. Bauer-Gottwein, "WHAT-IF: An open-source decision support tool for water infrastructure investment planning within the water-energy-food-climate nexus," *Hydrology and Earth System Sciences,* vol. 23, no. 10, pp. 4129-4152, 2019.

[12] C. Fant, Y. Gebretsadik, A. McCluskey and K. Strzepek, "An uncertainty approach to assessment of climate change impacts on the Zambezi River Basin," *Climatic Change,* vol. 130, pp. 35-48, 2015.

[13] R. Spalding-Fechera, B. Joyceb and H. Winklerc, "Climate change and hydropower in the Southern African Power Pool and Zambezi River Basin: System-wide impacts and policy implications," *Energy Policy,* vol. 103, pp. 84-97, 2017.

[14] Joint Global Change Research Institute, "GCAM v4.3 documentation: Global change assessment model (GCAM)," JGCRI, 2017.

[15] A. Thomson, K. Calvin, S. Smith, G. Kyle, A. Volke, P. Patel and J. Edmonds, "RCP4.5: A pathway for stabilization of radiative forcing by 2100," *Climatic Change,* vol. 109, no. 1-2, pp. 77-94, 2011.

[16] L. Clarke, K. Jiang, K. Akimoto, M. Babiker, G. Blanford, K. Fisher-Vanden, J.-C. Hourcade, V. Krey, E. Kriegler, A. Löschel, D. McCollum, S. Paltsev, S. Rose, P. R. Shukla and Tavoni, "Assessing transformation pathways," in *Climate Change 2014: Mitigation of Climate Change, Fifth Assessment Report of the Intergovernmental Panel on Climate Change*, New York, NY, Cambridge University Press, 2014.

[17] K. Calvin, B. Bond-Lamberty, L. Clarke, J. Edmonds, J. Eom, C. Hartin, S. Kim, P. Kyle, R. Link, R. Moss, H. McJeon, P. Patel, S. Smith, S. Waldhoff and M. Wise, "The SSP4: A world of deepening inequality," *Global Environmental Change,* vol. 42, pp. 284-296, 2017.

[18] D. van Vuuren, K. Riahi, K. Calvin, R. Dellink, J. Emmerling, S. Fujimori, S. KC, E. Kriegler and B. O'Neill, "The Shared Socio-economic Pathways: Trajectories for human development and global environmental change," *Global Environmental Change,* vol. 42, pp. 148-152, 2017.

[19] E. Kriegler, J. Edmonds and S. Hallegatte, "A new scenario framework for climate change research: the concept of shared climate policy assumptions," *Climatic Change,* vol. 122, pp. 401-414, 2014.

[20] K. Riahi, D. van Vuuren, E. Kriegler, J. Edmonds, B. O'Neill and S. Fujimori, "he shared socioeconomic pathways and their energy, land use, and greenhouse gas emissions implications: An overview," *Global Environmental Change,* vol. 42, p. 153–168, 2017.

[21] J. Lamontagne, P. Reed, R. Link, K. Calvin, L. Clarke and J. Edmonds, "Large Ensemble Analytic Framework for Consequence-Driven Discovery of Climate Change Scenarios," *Earth's Future,* p. 488– 504, 2018.

[22] X. Li, C. Vernon, M. Hejazi, R. Link, Z. Huang, L. Liu and L. Feng, "Tethys–A Python Package for Spatial and Temporal Downscaling of Global Water Withdrawals," *Journal of Open Research Software,* vol. 6, 2018.

[23] Z. Huang, M. Hejazi, Q. Tang, C. Vernon, Y. Liu, M. Chen and K. Calvin, "Global agricultural green and blue water consumption under future climate and land use changes," *Journal of Hydrology,* vol. 574, pp. 242-256, 2019.

[24] D. van Vuuren, J. Edmonds, M. Kainuma, K. Riahi, A. Thomson, K. Hibbard, G. Hurtt, T. Kram, V. Krey, J. Lamarque, T. Masui, M. Meinshausen, N. Nakicenovic, S. Smith and S. Rose, "The representative concentration pathways: an overview," *Climatic Change,* vol. 109, no. 5, 2011.

[25] C. Sadoff, D. Whittington and D. Grey, Africa's international rivers: an economic perspective, Washington, D.C.: The World Bank, 2003.

[26] R. Beilfuss, "Zambezi River Delta (Mozambique)," in *The Wetland Book*, M. G. P. R. D. N. Finlayson C., Ed., Dordrecht, Springer, 2016.

[27] World Bank, "The Zambezi River Basin. A Multi-Sector Investment Opportunities Analysis," World Bank, Washington, DC, 2010.

[28] M. Jeuland and D. Whittington, "Water resources planning under climate change: Assessing the robustness of real options for the Blue Nile," *Water Resources Research,* vol. 50, no. 3, pp. 2086-2107, 2014.

[29] J. J. S. Warner, E. Jones, M. Ansari and L. De Vries, "The Fantasy of the Grand Inga Hydroelectric Project on the River Congo," *Water,* vol. 11, no. 3, p. 407, 2019.

[30] K. Winemiller, P. Mcintyre, L. Castello, E. Fluet-Chouinard, T. Giarrizzo, S. Nam, I. G. Baird, W. Darwall, N. K. Lujan, I. Harrison, M. L. Stiassny, R. A. Silvano, D. B. Fitzgerald, F. M. Pelicice, A. A. Agostinho, L. C. Gomes and Al, "Balancing hydropower and biodiversity in the Amazon, Congo, and Mekong," *Science,* Vols. 351(6269),, no. 6269, pp. 128-129., 2016.

[31] D. Conway, E. van Garderen, D. Deryng, S. Dorling, T. Krueger, W. Landman, B. Lankford, K. Lebek, T. Osborn, C. Ringler, J. Thurlow, T. Zhu and C. Dalin, "Climate and southern Africa's water–energy–food nexus," *Nature Climate Change,* vol. 5, no. 9, pp. 837-846, 2015.

[32] ZAMCON, "Strategic Plan for the Zambezi watercourse 2018-2040," Zambezi River Basin Commission, Harare (Zimbabwe), 2019.

[33] R. Cervigni, R. Liden, J. Neumann and K. Strzepek, "Enhancing the Climate Resilience of Africa’s Infrastruc- ture: The Power and Water Sectors," World Bank, Washington, DC, 2015.

[34] BirdLife International, "World Database of Key Biodiversity Areas," 2018. [Online]. Available: www.keybiodiversityareas.org. [Accessed 2018 08 07].

[35] R. Beilfuss and D. dos Santos, "Patterns of hydrological change in the Zambezi Delta, Mozambique," in *Program for the Sustainable Management of Cahora Bassa Dam and the Lower Zambezi Valley*, 2001.

[36] C. Coello Coello, G. Lamont and D. V. Veldhuizen, Evolutionary Algorithms for Solving Multi-Objective Problems, New York, NY: Springer, 2007.

[37] A. Tilmant, L. Beevers and B. Muyunda, "Restoring a flow regime through the coordinated operation of a multireservoir system: The case of the Zambezi River basin," *Water Resources Research,* vol. 46, 2010.

[38] M. Rulli, A. Saviori and P. D’Odorico, "Global land and water grabbing," *Proceedings of the National Academy of Sciences,* vol. 110, no. 3, pp. 892-897, 2013.

[39] C. Zarfl, A. Lumsdon, J. Berlekamp, L. Tydecks and K. Tockner, "A global boom in hydropower dam construction," *Aquatic Sciences,* vol. 77, pp. 161-170, 2015.

[40] N. Graham, M. Hejazi, M. Chen, E. Davies, J. Edmonds, S. Kim, S. W. Turner, X. Li, C. R. Vernon, K. Calvin, F. Miralles-Wilhelm, L. Clarke, P. Kyle, R. Link, P. Patel, A. C. Snyder and M. Wise, "Humans drive future water scarcity changes across all Shared Socioeconomic Pathways," *Environmental Research Letters,* vol. 15, no. 1, 2020.

[41] L. Liu, M. Hejazi, G. Iyer and B. Forman, "Implications of water constraints on electricity capacity expansion in the United States," *Nature Sustainability ,* vol. 2, no. 3, pp. 206-213, 2019.

[42] D. McCollum, A. Gambhir, J. Rogelj and C. Wilson, "Energy modellers should explore extremes more systematically in scenarios," *Nature Energy,* vol. 5, no. 2, pp. 104-107, 2020.

[43] D. Schlosberg and L. Collins, "From environmental to climate justice: climate change and the discourse of environmental justice," *Wiley Interdisciplinary Reviews: Climate Change,* vol. 5, no. 3, pp. 359-374, 2014.

[44] N. Taconet, A. Méjean and C. Guivarch, "Influence of climate change impacts and mitigation costs on inequality between countries," *Climatic Change,* pp. 1-20, 2020.

Methods

We base our analysis on an integrated modeling approach that combines three main components (Supplementary Figure S12): (1) a strategic model of the Zambezi Watercourse; (2) the generation of climate scenarios that produced downscaled projections of precipitation and temperature, which are used as inputs for the hydrologic models of the Zambezi Watercourse sub-basin; (3) the generation of irrigation demand scenarios that produce downscaled projections of demands for the irrigation districts in the Zambezi Watercourse model.

Zambezi Watercourse model

The model of the Zambezi Watercourse (Supplementary Figure S12c) relies on a combination of conceptual and data-driven models, including the hydrologic model of the sub-catchments, the dynamic model of the reservoirs, and the irrigation diversions serving the agricultural districts located along the river (for details, see Supplementary Section S2).

The Ithezi-thezi, Victoria Falls, and Luangwa sub-basins are represented through the conceptual hydrologic model Hydrologiska Byrans Vattenbalansavdelning (HBV) [45], which simulate the soil water balance and subsequent rainfall-runoff processes. This model has been used extensively for climate change impact assessments [46, 47, 48], including previous research in the same basin [49]. The models were calibrated over the period 1981-1998 and validated over the 1998-2006 (in the case of Luangwa the periods 1981-1990 and 1996-2001 were used due to the presence of several gaps in the available timeseries). The average coefficient of determination in validation for the three HBV models is equal to 0.75 (for more details, see Supplementary Table S1).
The Shire sub-basin, which includes also Lake Malawi, is modeled by using of a data-driven artificial neural network reproducing the net inflows to the lake (i.e., inflows minus evaporation losses) coupled with a mass-balance equation reproducing the lake dynamics. The coefficient of determination of the combined model is equal to 0.63.

Precipitation data are taken from the Climate Hazard Group InfraRed Precipitation with Station (CHIRPS) gridded dataset [50], which provides daily timeseries starting in 1981 with a spatial resolution of 0.05°. Temperature data are instead taken from Observational Reanalysis Hybrid (OHR) gridded dataset, which provides daily timeseries of minimum and maximum temperature from 1981 to 2005 with a spatial resolution of 0.1° [51]. Lastly, streamflow data are from the Zambezi River Authority using the following gauging stations: Kafue Hook Bridge, Victoria Falls IN, Great East Road Bridge, and Mangochi.

The monthly dynamics of the main reservoirs, namely Ithezhi-tezhi, Kafue Gorge, Kariba, and Cahora Bassa, is described by the mass balance of the water volume stored in each reservoir. The release volume is determined by a nonlinear, stochastic function that depends on the release decision [52]. This function allows representing the effect of the uncertain inflows between the time at which the decision is taken (i.e., beginning of each month) and the time at which the release is completed (i.e., end of the month). The actual release might indeed not be equal to the decision due to existing legal and physical constraints on the reservoir level and release, including spills when the reservoir level exceeds the maximum capacity.

According to the monthly time-step of the model, the river reaches are modelled as plug-flow canals with negligible travel time and without any lamination effect. An exception is made for the Kafue Flats, an extensive floodplain where the river flows slowly for 250 km taking about two months from Ithezi-thezi to reach Kafue Gorge. Minimum environmental flow constraints protect the ecosystems at Victoria Falls and in the Kafue Flats: the diversion to the Victoria Falls power plant should ensure 250 m^3/s in the mainstream; the releases from Ithezi-thezi should guarantee a streamflow equal to 40 m^3/s (315 m^3/s in March) in the Kafue Flats [35].

The four reservoirs are connected to an associated hydropower plant. In addition, a run-of-the-river hydropower plant is in operation at Victoria Falls. The total installed capacity is 5.12 GW. The 7 agricultural districts are characterized by time-varying irrigation demands associated to a corresponding diversion channel that is regulated by a non-linear hedging rule [53]. The historical water demands are taken from [27], which specifies also the cultivated crops (i.e., mostly wheat and maize, except for the districts along the Kafue River that cultivates sugarcane) and the irrigation districts area is retrieved from the Global Map of Irrigation Areas by FAO AQUASTAT, which reports the areas equipped with irrigation in 2005 over a grid with spatial resolution of 0.083°.

Different objective functions representing the three components of the Water-Energy-Food Nexus were formulated though a participatory process involving key stakeholders active in the system, that participated in dedicated meetings called Negotiation Simulation Labs held during the DAFNE research project (see Supplementary Section S1).

The Water component of the Nexus is associated to the protection of the ecosystems in the Zambezi River Delta and is formulated as the environmental deficit with respect to a target pulse during the peak flow season [26, 37]. The Energy component of the Nexus is related to the total hydropower production obtained as the sum of the production in all the modeled hydropower plants. According to the Zambezi River Basin master plan [32] and considering that all these power plants are connected to the Southern African Power Pool where they export hydroelectric energy (based on International Energy Agency data https://www.iea.org/), the hydropower production is measured at the basin-wide scale, thus neglecting potential competition across countries. The Food component of the Nexus is captured by two distinct objectives: the first is the irrigation deficit, considered as a proxy for the food production, which formulated as the total average water supply deficit over all the irrigation districts; the second is the variance of the average squared water supply deficits across the districts to avoid unbalanced water allocations.

The coordinated operation of the four reservoirs and 7 diversion channels is determined by a closed-loop operating policy [54] that depends on the month of the year, the four reservoir storages, and the total previous month inflow. This allows simulating sequences of control actions that optimally respond to the evolving system conditions, thus representing an upper-bound solution that removes the myriad of institutional and geophysical factors that can cause actual operations to deviate from optimal rules [55]. The optimal policies are designed via evolutionary multi-objective direct policy search method [56], a Reinforcement Learning approach that combines direct policy search, nonlinear approximating networks, and multi-objective evolutionary algorithms. The policies are defined as Gaussian radial basis functions [57] and the policy parameters are optimized using the self-adaptive Borg Multi-Objective Evolutionary Algorithm [58], a combination that has been demonstrated to be effective in solving these types of multi-objective policy design problems for large-scale water systems [59]. These adaptive operating policies are applied through the simulation period. Accounting for potential changes to institutions or values that introduce new objectives, values, constraints, or allowable actions to compensate objectives suffering persistent deficits and to adapt the system operations to the projected changes in climate and society is beyond the scope of this work, and remains a grand challenge in water resources and socio-environmental systems modeling [60, 61].

Generation of climate scenarios

Climate projections (Supplementary Figure S12a) are obtained from the CORDEX project [62]. Specifically, we use a total of 9 scenarios that include 3 Representative Concentration Pathways, namely RCP2.6, RCP4.5, and RCP8.5, as simulated by three different combinations of global climate models (GCMs) dynamically downscaled by a regional climate model (RCM), which provides simulated trajectories of precipitation and temperature with a spatial resolution of 0.44°: the MPI-ESM-LR GCM downscaled using the RCA4 RCM, and the ICHEC-EC-EARTH GCM downscaled by either the RCA4 or the RACMO RCMs. Despite the incompleteness of CORDEX-Africa RCM-GCM matrix, these combinations allow exploring the uncertainties associated to both global and regional climate models. As CORDEX Africa does not provide multiple downscaled realizations for the same GCM-RCM model combination, in this work we did not explore the uncertainties related to internal model variability. However, previous studies [63] showed that results based on "one simulation one vote" approach are often robust regardless of the choice of the specific RCMs or GCMs. In the future, it would be worthwhile to investigate the sensitivity of our results to the climate projections considered and more broadly explore the climate models' dynamics by using a larger ensemble of scenarios, possibly including downscaled CMIP6 projections when they become available.
We further bias-adjusted these scenarios using a time-varying quantile mapping technique to match the cumulative density function (CDF) of the RCM simulations over the control period (1981-2005) with the CDF of the observations, generating a correction function depending on the day of the year and the quantile of the distribution. The correction function is then used to unbias day by day and quantile by quantile the considered variable over the projection period (2006-2100). The pattern of change of the resulting trajectories (Supplementary Figures S4 and S5) seems to be primarily driven by the considered RCP scenario, while the differences introduced by the three GCM-RCM combinations are less outstanding (see also the indices from the Expert Team on Climate Change Detection and Indices (ETCCDI [64]) reported in Supplementary Figure S9). Lastly, the downscaled projections of trajectories of precipitation and temperature are used as inputs to the local hydrologic models for generating streamflow projections (Supplementary Figure S6).

Generation of irrigation demand scenarios

The socio-economic scenarios used in this study (Supplementary Figure S12b) were developed by [21] through a factorial sampling of the Shared Socio-economic Pathways (SSPs) and Shared Policy Assumptions (SPAs). That work aggregated the SSP assumptions into six categories: socio-economics (population, GDP), changes in energy demand (transportation, building, industrial), agricultural productivity and dietary trends, fossil fuel extraction costs, renewable energy costs, and carbon capture and sequestration costs. Within each category, discrete sampling levels tied to the SSP quantification by [17] were defined. Scenarios were generated through a full factorial combination of all sampling levels across all uncertainty categories. Three long-term CO2 price trajectories were used to simulate different levels of global emissions reductions: a no-tax business as usual case, a low-tax case ($10/tonne of CO2 in 2020, increasing at 5% per year), and a high-tax case ($25/tonne of CO2 in 2020, increasing at 5% per year). Policy implementation uncertainty, as described in the Shared Policy Assumptions (SPAs, [19]) was also sampled (Supplementary Table S2). Specifically, whether a delay in the universal adoption of the CO2 price would occur, and the extent (geographic and level) to which LUC emissions would be priced. In total, 33,750 global change scenarios were generated and simulated using the Global Change Analysis Model (GCAM).

GCAM is a global integrated assessment model that pairs a representation of various natural systems (primarily the climate) with representations of various human systems, including the agricultural, energy, transportation, and building sectors. GCAM was one of four models used to develop the RCPs [15], one of five models used to quantify the SSPs [17], and was used in the IPCC's fifth assessment report [16]. GCAM divides the world into 32 energy-economic zones, which are further sub-divided into 233 river basins, and 283 agro-ecological zones [14]. The model is modular, allowing sectors in different regions and basins to represented with varying levels of detail. Sectors and regions are linked by markets for energy and agricultural goods. This linkage allows for the incorporation of economic teleconnections in regional resource analyses. For instance, the impact of population growth or technological innovation in one region on agricultural water consumption in another can be quantified. GCAM is a partial equilibrium model, in which prices are

adjusted in each simulation period such that supply equals demand for all goods in all markets in all regions.

Factors like population growth, changing preferences, and per capita income growth will impact the global demand for various crops. Regional differences in agricultural productivity, land availability, and LUC emissions policies determine regional crop production levels in each of the 33,750 scenarios developed by [21]. This regional crop production is divided into irrigated and rainfed production, and the corresponding water consumption based on fixed ratios (see Supplementary Section S3) is then spatio-temporally downscaled to monthly crop irrigation demands (Supplementary Figure S10) on a 0.5-degree grid using the Tethys model [22]. The resulting gridded irrigation demands enter directly to the Zambezi Watercourse Model. In the future, it would be worthwhile to investigate the impacts on the Zambezi Watercourse dynamics of projected non-agricultural demands that are not considered in this study. As most SSP scenarios include an increase in the global population by 2100, most scenarios in Figure 3b see an increase in global crop water consumption: there are more people to feed. The magnitude of the global increase is tied to many factors (population, technology, etc.), but the distribution of the increase is heavily tied to the nature of the mitigation policy. Worlds with a regionally differentiated LUC emissions regime will concentrate new agricultural production in regions where LUC emissions are not priced, and sufficient land is available. Under the SPA assumptions employed in this study, that includes much of Africa (see also [65]).

A promising direction of future work would be assessing the impacts on the WEF systems in the Zambezi Watercourse of other climate change mitigation options, including afforestation [66], power plant expansions [11], or alternative carbon price regimes [65].
Notably, a carbon price regime not considered here is a fossil fuel and industrial carbon tax (FFICT), that applies no price to land use change emissions. The impact of such a regime on tradeoffs in the Zambezi are difficult to anticipate. Recent work suggests that an FFICT would encourage agricultural global extensification, in part for biofuels and in part irrigated, while policies including land use change emissions encourage greater water use through intensive irrigation [65].

Generation of interdependent scenarios

We generated an ensemble of interdependent scenarios through an a posteriori coupling of the irrigation demand scenarios with the climate projections based on the 2100 radiative forcing simulated by GCAM and used as starting point for the generation of the climate scenarios. Specifically, we associated to the three RCP projections the scenarios of irrigation demands generated by a simulation of GCAM returning a value of radiative forcing in 2100 within a window of 0.2 W/m^2 centered in 2.6, 4.5, and 8.5 W/m^2, respectively (Supplementary Figure S3). Notably, none of the GCAM simulations produces a forcing value compatible with the projections of RCP2.6. This is because [21] considered relatively moderate carbon-price trajectories, while high carbon prices are needed to achieve RCP2.6 forcing in most sampled worlds. We therefore associate this climate projection with the irrigation demand scenarios characterized by the smallest forcing values simulated by GCAM. The coupling of climate and socio-economic projections substantially reduced the number of the irrigation demand scenarios: starting from the 33,750-member ensemble, the resulting ensemble of interdependent scenario includes 2,439 demand scenarios for each GCM-RCM combinations, yielding a total of 7,317 ensemble members.
The nature of the coupling in this analysis will introduce some small inconsistencies as the exact forcing trajectories produced by the socio-economic scenarios will deviate somewhat from the RCP trajectories (Supplementary Figure S3). In this study, this means that the water availability is computed using slightly different global forcing levels than the irrigation demand. However, for such small forcing deviations, GCM uncertainty is more impactful on river discharge than forcing uncertainty [67]. Relaxing the strict coupling allows a richer exploration of the drivers of irrigation demand than is typically afforded.

Data Availability

All climate data are freely available at the following websites: historical precipitation https://chc.ucsb.edu/data/chirps, historical temperature http://hydrology.princeton.edu/data.metdata_africa.php, projected precipitation and temperature http://www.csag.uct.ac.za/cordex-africa/ (see Supplementary Table S3). Data about the socio-economic scenarios produced by GCAM simulations are available in the Github repository https://github.com/JRLamontagne/Factorial_SSP-SPA_Exploration.
Bias-adjusted climate projections and corresponding simulated streamflow are available in the open source repository https://doi.org/10.5281/zenodo.5726941 [68].
All the historical hydrologic data on the Zambezi River basin are from the Zambezi River Authority (ZRA) and were collected during the DAFNE project (http://dafne-project.eu/). They are protected by a nondisclosure agreement with ZRA.

Code Availability

The code of the HBV models is available in the open source repository https://doi.org/10.5281/zenodo.5726941 [68].
Because the Zambezi Watercourse model described in Supplementary Section S2 contains sensitive hydrologic data, along with hydropower plant characteristics from ZRA, Zambia Electricity Supply Corporation (ZESCO), and Hidroeléctrica de Cahora Bassa (HCB), it cannot be made public. The simulation outputs and the code for generating the figures can be however found in the open source repository https://doi.org/10.5281/zenodo.5726941 [68].

References

45. G. Lindström, B. Johansson, P. M., M. Gardelin and S. Bergström, "Development and test of the distributed HBV-96 hydrological model," *Journal of Hydrology,* vol. 201, no. 1-4, pp. 272-288, 1997.
46. M. Akhtar, N. Ahmad and M. Booij, "Use of regional climate model simulations as input for hydrological models for the Hindukush-Karakorum-Himalaya region," *Hydrology and Earth System Sciences,* vol. 13, pp. 1075-1089, 2009.
47. S. Bergström, A. Johan, V. Noora, V. Bertel, E. Bergur, J. Sveinbjörn, K. Liga, K. Jurate, M. Diana and B. Stein, "Modelling Climate Change Impacts on the Hydropower System; Climate Change and Energy Systems Impacts, Risks and Adaptation in the Nordic and Baltic Countries," Nordic Council of Ministers, Copenhagen, Denmark, 2012.
48. A. Vrochidou, I. Tsanis, M. Grillakis and A. Koutroulis, "The impact of climate change on hydrometeorological droughts at a basin scale," *Journal of Hydrology,* vol. 476, pp. 290-301, 2013.
49. B. Hamududu and A. Killingtveit, "Hydropower production in future climate scenarios; the case for the Zambezi River," *energies,* vol. 9, no. 502, 2016.
50. C. Funk, P. Peterson and M. Landsfeld, "The climate hazards infrared precipitation with stations - a new environmental record for monitoring extremes," *Scientific Data,* vol. 2, 2015.
51. N. Chaney, J. Sheffield, G. Villarini and E. Wood, "Development of a high-resolution gridded daily meteorological dataset over sub-Saharan Africa: spatial analysis of trends in climate extremes," *Journal of Climate,* vol. 27, no. 15, pp. 5815-5835, 2014.
52. R. Soncini-Sessa, A. Castelletti and E. Weber, Integrated and participatory water resources management: Theory, Amsterdam: Elsevier, 2007.
53. A. Celeste and M. Billib, "Evaluation of stochastic reservoir operation optimization models," *Advances in Water Resources,* vol. 32, no. 9, pp. 1429-1443, 2009.
54. A. Castelletti, F. Pianosi and R. Soncini-Sessa, "Water reservoir control under economic, social and environmental constraints," *Automatica,* vol. 44, no. 6, pp. 1595-1607, 2008.
55. F. Bertoni, A. Castelletti, M. Giuliani and P. Reed, "Discovering dependencies, trade-offs, and robustness in joint dam design and operation: An ex-post assessment of the Kariba dam," *Earth's Future,* vol. 7, p. 1367–1390, 2019.

56. M. Giuliani, A. Castelletti, F. Pianosi, E. Mason and P. Reed, "Curses, tradeoffs, and scalable management: Advancing evolutionary multi-objective direct policy search to improve water reservoir operations," *Journal of Water Resources Planning and Management,* vol. 142, no. 2, 2016.
57. L. Busoniu, D. Ernst, B. De Schutter and R. Babuska, "Cross-entropy optimization of control policies with adaptive basis functions," *IEEE Transactions on Systems Man Cybernetics,* vol. 41, no. 1, pp. 196-209, 2011.
58. D. Hadka and P. Reed, "Borg: An auto-adaptive many-objective evolutionary computing framework," *Evolutionary Computation,* vol. 21, no. 2, pp. 231-259, 2013.
59. M. Giuliani, J. Quinn, J. Herman, A. Castelletti and P. Reed, "Scalablemultiob- jective control for large-scale water resources systems under uncertainty," *IEEE Transactions on Control Systems Technology,* vol. 26, no. 4, pp. 1492-1499, 2018.
60. G. Blöschl, M. Bierkens, A. Chambel, C. Cudennec, G. Destouni and A. Fiori, "Twenty-three unsolved problems in hydrology (UPH)–a community perspective," *Hydrological sciences journal,* vol. 64, no. 10, pp. 1141-1158, 2019.
61. S. Elsawah, T. Filatova, A. Jakeman, A. Kettner, M. Zellner, I. Athanasiadis, S. Hamilton, R. Axtell, D. Brown and J. Gilligan, "Eight grand challenges in socio-environmental systems modeling," *Socio-Environmental Systems Modelling,* vol. 2, pp. 16226-16226, 2020.
62. F. Giorgi, C. Jones and G.R. Asrar, "Addressing climate information needs at the regional level: the cordex framework," *World Meteorological Organization (WMO) Bulletin,* vol. 58, no. 3, 2009.
63. A. Dosio, R. Jones, C. Jack, C. Lennard, G. Nikulin and B. Hewitson, "What can we know about future precipitation in Africa? Robustness, significance and added value of projections from a large ensemble of regional climate models.," *Climate Dynamics,* vol. 53, pp. 5833-5858, 2019.
64. X. Zhang, L. Alexander, G. Hegerl, P. Jones, A. Tank and T. Peterson, "Indices for monitoring changes in extremes based on daily temperature and precipitation data," *Wiley Interdisciplinary Reviews: Climate Change,* vol. 2, no. 6, pp. 851-870, 2011.
65. F. Dolan, J. Lamontagne, R. Link, M. Hejazi, P. Reed and J. Edmonds, "Evaluating the economic impact of water scarcity in a changing world," *Nature Communications,* vol. 12, 2021.
66. A. Mosnier, P. Havlik, M. Obersteiner, K. Aoki, E. Schmid, S. Fritz, I McCallum, S. Leduc, “Modeling impact of development trajectories and a global agreement on reducing emissions from deforestation on Congo Basin forests by 2030”, *Environmental and Resource Economics*, vol. 57, pp. 505-525, 2014
67. F. Hattermann, T. Vetter, L. Breuer, B. Su, P. Daggupati and C. Donnelly, "Sources of uncertainty in hydrological climate impact assessment: a cross-scale study," *Environmental Research Letters,* vol. 13, no. 1, p. 015006, 2018.
68. M. Giuliani, & J.R. Lamontagne. (2021). First release of ZambeziWatercourse_GCAM code (v1.0-alpha). Zenodo. https://doi.org/10.5281/zenodo.5726941

539

540